Novel Immunological Markers of Intestinal Impairment Indicative of HIV-1 Status and/or Subclinical Atherosclerosis

Etiene Moreira Gabriel[1,2], Jonathan Dias[1,2], Ramon Edwin Caballero[2,3], Tomas Wiche Salinas[1,2], Manon Nayrac[2], Abdelali Filali-Mouhim[4], Carl Chartrand-Lefebvre[2,5], Jean-Pierre Routy[6,7], Madeleine Durand[2,8], Mohamed El-Far[2], Cécile Tremblay[1,2], and Petronela Ancuta[1,2*]

[1]Département de microbiologie, infectiologie et immunologie, Faculté de Médecine, Université de Montréal, Montréal, Québec, Canada

[2]Centre de Recherche du CHUM, Montréal, Québec, Canada

[3]Department of Microbiology & Immunology, School of Biomedical Sciences, McGill University, Montreal, Quebec, Canada

[4]Centre de recherche, Institut universitaire de gériatrie de Montréal, Montréal, Québec, Canada

[5]Département de radiologie, radio-oncologie et médecine nucléaire, Faculté de Médecine, Université de Montréal, Montréal, Québec, Canada

[6]Chronic Viral Illness Service and Division of Hematology, Research Institute of the McGill University Health Centre, Montreal, QC, Canada

[7]McGill University Health Centre, Glen site, Montreal, QC, Canada

[8]Département de Médecine, Faculté de Médecine, Université de Montréal, Montréal, Québec, Canada

Email addresses of the authors: etiene.moreira.gabriel@umontreal.ca; jonathan.dias@umontreal.ca; ramon.caballero@mail.mcgill.ca; tomas.raul.wiche.salinas@umontreal.ca; manon.nayrac@umontreal.ca; alifilali2009@gmail.com; carl.chartrand-lefebvre@umontreal.ca; jean-pierre.routy@mcgill.ca;

madeleine.durand@umontreal.ca; mohamed.el.far.chum@ssss.gouv.qc.ca;

c.tremblay@umontreal.ca; and petronela.ancuta@umontreal.ca

*, **Corresponding author mailing address**:

Petronela Ancuta, Centre de Recherche du CHUM, 900 rue Saint-Denis, Tour Viger R, Room R09.416, Montréal, Quebec H2X 0A9, Canada; Phone: +1 514-890-8000, extension #35744;

e-mail: petronela.ancuta@umontreal.ca

Abstract word count: 250 words

Text word count: 5410 words (Introduction, Methods, Results, Discussion)

Figures: 4

Tables: 3

Supplemental Figures: 8

Supplemental files: 1

Supplemental Tables: 3

ABSTRACT

Antiretroviral therapy (ART) controls HIV-1 replication in people with HIV-1 (PWH), but immunological restauration at mucosal barrier surfaces is not achieved. This fuels microbial translocation, chronic immune activation, and increased comorbidities, including cardiovascular disease (CVD). Here, we sought to identify novel markers of mucosal barrier impairment in the blood to predict the HIV and/or CVD status. Flow cytometry was used to characterize CD326/EpCAM^{+} intestinal epithelial cells (IEC); CD4^{+} T-cells; CD8^{+} and CD4^{+} intraepithelial lymphocytes (IELs); and subsets of CD4^{+} T-cells expressing Th17 (CCR6) and gut-homing (Itgβ7) markers. To this aim, we collected peripheral blood mononuclear cells (PBMCs) from 42 ART-treated PWH (HIV^{+}) and 40 uninfected participants (HIV^{-}) from the Canadian HIV and Aging Cohort Study (CHACS). Both groups were categorized based on the presence of coronary atherosclerotic plaques measured by CT scan angiography as total plaque volume (TPV, mm^{3}).

Our findings associate the HIV-1 status with increased frequencies of circulating CD326^{+} IEC; CD326^{+}CD4^{+} T-cells with activated (CD69^{+}HLA-DR^{+}) and gut-homing (ItgαE^{+}CCR6^{+}CCR9^{+}) phenotypes, CCR6^{+}Itgβ7^{-}CD4^{+} T-cells; and decreased frequencies of CD8^{+} IELs. Logistic regression analyses confirmed the predictive capacity of the above cellular markers regarding HIV status. Spearman correlation revealed a positive correlation between TPV and CCR6^{+}Itgβ7^{-} and CCR6^{+}Itgβ7^{+} CD4^{+} T-cell frequencies.Together, these results highlighted significant immune dysregulation and persistent mucosal barrier alterations despite effective viral suppression by ART and linked the abundance of CCR6^{+}Itgβ7^{+} and CCR6^{+}Itgβ7^{-} CD4^{+} T-cells to increased atherosclerotic plaque burden. Thus, strategies targeting the gut-immune axis restoration may reduce CVD onset and improve long-term health outcomes in PWH.

Key words: HIV, CVD, gut-homing, CCR6, epithelial cells, CD326, EpCAM, IELs.

INTRODUCTION

HIV-1 affects an estimated 39.0 million individuals globally, with approximately 1.3 million new incidences reported in 2022 [1]. While antiretroviral therapy (ART) has significantly improved the lives of people with HIV-1 (PWH), transforming it into a manageable chronic condition, treatment is not curative [2, 3]. Consequently, ART-treated PWH experience premature aging and increased risk of developing non-AIDS comorbidities, such as cardiovascular disease (CVD) [4-6]. Therefore, new efforts are required to find solutions for the current medical challenges faced by PWH, even in countries where ART is efficiently available.

HIV-1 infection provokes profound immunological alterations leading to inadequate mucosal barrier functions. This can result in cells displaying modified immune phenotypes related to inflammation and cell activation [7, 8]. Notably, the expression of HLA-DR, especially on $CD4^+$ T-cells, is identified as a sign of overt immune activation and a critical marker of HIV-1 disease progression [9, 10]. The gut-associated lymphoid tissues (GALT) represent the primary location for $CD4^+$ T-cell depletion during the acute phase of HIV-1 infection and also constitute an important site for HIV-1 reservoir persistence during the chronic phase [11-13]. ART initiation promptly decreases HIV-1 viral loads and results in the normalization of $CD4^+$ T-cell counts in the bloodstream. However, even in cases where viral suppression occurs and circulating $CD4^+$ T-cell counts are restored, PWH continue to exhibit elevated $CD8^+$ T-cell counts, resulting in persistently imbalanced CD4/CD8 ratios, demonstrating immune dysfunction. A low CD4/CD8 ratio can predict morbidity and mortality [14, 15]. In addition, the replenishment of the $CD4^+$ T-cell pools within the GALT progresses slowly and is less complete than in the peripheral blood [16]. This inadequate recovery of GALT-infiltrating $CD4^+$ T-cells leads to a breach in the

epithelial cell barrier, promoting microbial translocation and triggering immune activation [12, 17, 18]. These events, uncontrolled by ART, are documented to fuel a state of chronic inflammation and immune activation facilitating the occurrence of non-AIDS comorbidities in ART-treated PWH, including cardiovascular disease (CVD) and premature aging [4-7, 19-21].

Effective communication between intestinal epithelial cells (IEC) and immune cells is crucial for maintaining mucosal homeostasis in its capacity to fight pathogens at barrier surfaces [22, 23]. Th17-polarized CD4+ T-cells are fundamental for sustaining gut immunity, significantly aiding in maintaining epithelial integrity and functionality [24, 25]. Consequently, the deficit in Th17 cells profoundly alters the GALT barrier functions, leading to a compromised epithelium and chronic systemic inflammation [11, 24, 26]. Pioneering studies documented that HIV-1 infection is associated with changes in the expression of the gut-homing molecule integrin α4β7 on the peripheral $CD4^+$ T-cells [27-29] and that the expression of integrin α4β7 on blood $CD4^+$ T-cells mirrors events taking place in the gut [30, 31]. Since the integrin $\alpha4\beta7^+$ $CD4^+$ T-cell subset predominantly consists of Th17 cells [32], their capacity to migrate into the GALT justifies why $CCR6^+\alpha4\beta7^+$ Th17 cells are selectively targeted by HIV-1 for infection [27, 33-36]. Indeed, integrin α4β7 has been reported as a marker of $CD4^+$ T-cells highly permissive to HIV-1 infection [36, 37]. Nevertheless, we demonstrated that CD4+ T-cells expressing the Th17 marker CCR6 are highly permissive to HIV-1 infection regardless of the expression of integrin α4β7 [38]. In addition, our group and others have demonstrated that Th17 cells are major HIV-1 infection targets, especially due to their relatively high expression of HIV-1 permissiveness factors [12, 24, 39, 40]. Consistently, we demonstrated that retinoic acid promoted integrin α4β7 expression in both $CCR6^+$ and CCR6- $CD4^+$ T-cells, but increased HIV-1 replication and

outgrowth was mainly observed in RA-treated CCR6^{+} T-cells [34]. More evidences underscore how cellular immune activation is linked to the migration and subsequent depletion of Th17 cells in the gut of PWH [10, 12, 41]. In addition to Th17 cells, other T-cell subsets important for the maintenance of gut immunity include the intraepithelial lymphocytes (IELs), a subset marked by the expression of ItgαE/CD103 [42, 43]. Importantly, IELs are tissue-resident T-cells that usually do not recirculate in the blood [44, 45], with functional alterations in IELs reported during HIV-1 infection [46, 47].

The epithelial cell-adhesion molecule, EpCAM (CD326), is a specific marker of epithelial cells [48-50]. In the clinical context, this molecule holds significant relevance in oncology, identifying circulating tumor cells, validating their epithelial origin, and potentially replacing invasive tumor biopsies [50-52]. Circulating CD326^{+} epithelial cells were also reported in the context of autoimmune intestinal inflammation [53-55]. The "*liquid biopsy*" concept is now proposed to be extended to infectious diseases associated with an impaired intestinal epithelial barrier [56-58], but its validity in PWH remains to be explored.

Considering all this knowledge, we hypothesized that EpCAM^{+} epithelial cells and IELs could recirculate in the peripheral blood as a sign of gut barrier disruption in HIV-1 infection, and their presence in the blood, together with alterations in circulating CD4^{+} T-cell subsets expressing gut-homing markers, may be indicative of the HIV-1 status and subclinical CVD. In an effort to identify a novel blood immunological signature indicative of intestinal impairment and CVD development in ART-treated PWH, in this study, we had access to frozen PBMC samples from HIV-uninfected controls and ART-treated PWH included in the Canadian HIV and Aging Cohort

Study (CHACS), with and without subclinical atherosclerosis determined by Computed Tomography Scan (CT Scan) measurement of the coronary artery atherosclerotic plaque volume, as we previously reported [59, 60]. Polychromatic flow cytometry was used to monitor the frequency of circulating $CD326^+$ EC, IEL subsets, and $CD4^+$ T-cell subsets expressing gut-homing and activation markers. Together our findings reveal HIV-mediated immune alterations in the peripheral blood of PWH correlated to the presence of subclinical atherosclerotic plaque, thus, linking impaired gut-homing and exacerbated activation of $CD4^+$ T-cells to CVD development.

MATERIAL AND METHODS

Study Participants

The Canadian HIV and Aging Cohort Study (CHACS) has been described in previous publications [59, 61-63]. In summary, the inclusion criteria for the cardiovascular imaging subset of the CHACS cohort required participants to be over 40 years old, have a 10-year CVD risk as determined by the Framingham Risk Score (FRS – which calculates risk based on factors such as age, cholesterol levels, systolic blood pressure, smoking status, and diabetes status) ranging from 5-20%, and have no clinical diagnosis of CVD. Participants with renal impairment or a known hypersensitivity to contrast agents were excluded from the study. Here, we used PBMCs from 82 CHACS participants, of whom n=42 were ART-treated PWH and n=40 were HIV-uninfected participants. The clinical parameters of the study participants are depicted in Tables 1-2. Further stratification of both groups was conducted based on the presence or absence of subclinical atherosclerotic plaque on CCTA, determined by total plaque volume (TPV), measured in cubic millimeters (mm^3 equal to or greater than zero), as we previously reported [59, 60].

Ethical statement

The collection of peripheral blood from the participants was conducted in compliance with the Declaration of Helsinki. This research received approval from the Centre de Recherche du CHUM, Montréal, Québec, Canada (#CE.11.063). Written informed consents were obtained from all participants.

Blood collection and phenotypic analysis

Peripheral blood mononucleated cells (PBMCs) were isolated by Ficoll density centrifugation from peripheral blood collected by venipuncture on EDTA Vacutainer tubes. PBMCs were frozen in DMSO 10% FBS until use. Thawed PBMCs were stained with the following fluorochrome-conjugated antibodies: CD3 (AF700), CD45 (APC-H7), CD56 (PerCP-Cy5.5), CD69 (BV711), TCRαβ (BUV563), TCRγδ (BUV395), CD8αβ (RY586), CD8αα (BB515), CD33 (BV480), CD49d/Itgα4 (PE-CF594), Itgβ7 (BUV737), CD103/ItgαE (BUV805), CD196/CCR6 (BUV661), and CD199/CCR9 (APC) (BD Biosciences, Franklin Lakes, NJ, USA); CD4 (BV421), HLA-DR (BV785), CD326/EpCAM (BV650), CD19 (PerCP-Cy5.5) and CD66b (PerCP-Cy5.5; BioLegend, San Diego, California, USA). The fixable Viability Stain 575V (BV570; BD Biosciences) was used to exclude dead cells from the analysis. Phenotypic analysis was performed by flow cytometry using a FACSymphony™ A5 Cell Analyzer, (BD Biosciences) and FlowJo software (Tree Star, Ashland, Oregon, USA).

Statistical analysis

The Shapiro-Wilk test was employed to evaluate whether continuous variables followed a normal distribution. Normally distributed continuous variables were described using mean and standard deviation, whereas not normally distributed variables were described using median and interquartile range (IQR). A t-test was used for comparing two groups of normally distributed variables, while the Mann-Whitney test was used for comparing variables not normally distributed, using the GraphPad Prism 8 software (Dotmatics, Boston, Massachusetts, USA). Fisher's Exact Test was used to test if an association existed between two categorical variables. To assess the effect of potential confounding factors on the association between the circulating

cell subsets and the HIV status and the presence or absence of coronary plaque within HIV^+ individuals, logistic regression analyses were implemented in R [64]. First, univariate and multivariate logistic regression models were compared to study the contribution of the immune subset alone and in the presence of potential confounding factors (BMI, TPV, and LDL). The confounding effect was estimated by the measure of the association, quantified using the odds ratio (OR) before and after adjusting. A change in the estimated association measure of less than 10% was used to exclude confounders, while a change of more than 30% identified a large confounding bias [65, 66]. P-value adjustments for multiple testing hypotheses were performed according to the method of Benjamini and Hochberg [67], which controls the false discovery rate with adjusted p-value cutoffs of 0.05.

RESULTS

Clinical and laboratory characteristics of the study participants

The HIV^+ (n=42) and HIV^- (n=40) participants from the CHACS included in the cardiovascular imaging subgroup were categorized in TPV^+ and TPV^-, based on the presence or the absence of coronary atherosclerotic plaque. TPV was measured using coronary artery CT Scan, as we previously reported [60, 61]. Detailed demographic and clinical information on study participants are included in Table 1. Briefly, HIV^+ *versus* HIV^- participants were similar regarding age (mean 54.2 *versus* 54.6 years old), male sex (95% *versus* 84%), and Framingham risk score (FRS; median 9 *versus* 10). HIV^+ participants presented lower body mass index (BMI; median 24.62 *versus* 27.22 Kg/m^2; p=0.005). Smoking habits tended to be more prevalent among HIV^+ compared to HIV^- participants, but differences did not reach statistical significance (p=0.158). Among TPV^+ participants, TPV values were significantly higher in HIV^+ compared to HIV^- groups (median 851.7 *versus* 143 mm^3; p<0.0001). The HIV^+ and HIV^- groups presented statistically similar levels of D-dimers (median 353.5 *versus* 327.3 μg/L), fibrinogen (median 3.26 *versus* 2.92 G/L), HDL (median 1.23 *versus* 1.31 mmol/L), and triglycerides (median 1.87 *versus* 1.60 mmol/L); however, HIV^+ participants had lower levels of LDL than the HIV^- counterparts (median 2.75 *versus* 3.2 mmol/L; p=0.046). The latter observation can be explained by the fact that a higher percentage of HIV^+ participants were undergoing statin treatment (43% [18 of 42] compared to 15% [6 of 40]; p=0.007).

Detailed clinical and laboratory parameters in HIV^+ participants grouped based on the presence (TPV^+) or the absence (TPV^-) of plaque are included in Table 2. Among HIV^+ participants, the TPV^+ and TPV^- groups were statistically similar regarding age (mean 54.8 *versus* 53.7 years

old), male sex (100% *versus* 90.5%), and body mass index (BMI; median 24 *versus* 25.4 Kg/m^2). Smoking habits (p=0.0003) and FRS (median 12.2 *versus* 8.5; p=0.039) were higher among TPV$^+$ in comparison to TPV$^-$ participants. Statistically significant differences were observed between the TPV$^+$ and TPV$^-$ groups concerning plasma levels of D-dimer (median 375.5 *versus* 325.0 μg/L; p=0.049), while differences in Fibrinogen (median 3.6 *versus* 2.8 G/L), LDL (median 2.6 *versus* 2.9 mmol/L), HDL (median 1.24 *versus* 1.23 mmol/L), and triglycerides (median 2.29 *versus* 1.45 mmol/L) values did not reach statistical significance. Also, TPV$^+$ and TPV$^-$ HIV$^+$ participants presented similar levels of Cytomegalovirus (CMV) co-infection (92.3% *versus* 93.75%), duration of HIV infection (median 20.33 *versus* 17.51 years), duration of ART (mean of 16.7 *versus* 12.8 years), nadir CD4 (median 240 *versus* 242 xE9/L), and CD4 counts (mean 44% *versus* 48%).

Immune profile alterations indicative of HIV and subclinical CVD status

HIV infection can lead to a compromised intestinal epithelium and an altered functional profile of infiltrating immune cells, events associated with inflammation, perturbed gut-homing, and/or overt immune activation [7, 8, 12]. We hypothesized that HIV-specific alterations of the gut barrier functionality can be reflected in the peripheral blood of PWH. For this, PBMCs from HIV$^+$ and HIV$^-$ study participants, TPV$^+$ and TPV$^-$, were analyzed for the presence of hematopoietic CD45$^+$ and non-hematopoietic CD45$^-$ cells (Supplemental Figure 1). Among CD45$^+$ cells, T-cells lacking the lineage markers CD19 (B cells), CD56 (NK cells), CD66b (neutrophils), and CD33 (myeloid cells), but expressing CD3 (T-cells) were further analyzed for the expression of CD4 (CD4$^+$ T-cells) and CD8αβ (CD8$^+$ T-cells) (Supplemental Figure 1). As expected, our results showed statistically significant decreased and increased numbers of CD4$^+$

T-cells and $CD8^+$ T-cells, respectively, in HIV^+ compared to HIV^- participants, as well as decreased CD4/CD8 ratios (Supplemental Figure 2A). Aiming to investigate if there was a relationship between these parameters and the presence of plaque, we found that $CD4^+$ and $CD8^+$ T-cell numbers, as well as CD4/CD8 ratios, were similar regardless of the presence of plaque (Supplemental Figure 2B). For the HIV^- but not HIV^+ group the CD4/CD8 ratios correlated positively with age (Supplemental Figure 2C) and TPV (Supplemental Figure 2D), indicative of immunological alterations linked to increased CVD risk occurring regardless of aging in the HIV^+ group.

Frequency of circulating $CD326^+$ EC in relationship with the HIV infection and subclinical atherosclerosis status

Preliminary studies performed on a small cohort of ART-treated PWH (HIV^+; n=16; all men; median age: 54 years old; median CD4 counts: 679 cells/µl; median time since infection: 20 years; median time on ART: 7 years) and HIV-uninfected controls (HIV^-; n=5, 3 male; median age: 59 years old; median CD4 counts: 750 cells/µl), pointed to a tendency for increased frequencies of circulating $CD326^+$ EC in HIV^+ compared to HIV^- participants (median frequency: 0.045% *versus* 0.0095% within live cells; Mann-Whitney p=0.0752; Supplemental Figure 3). These results prompted us to assess the frequency of peripheral blood $CD326^+$ EC in the current cohort (Tables 1-2), in relationship with HIV and atherosclerosis status. $CD326^+$ EC were identified as non-hematopoietic $CD45^-$ cells lacking the expression of CD33, CD19, CD56 and CD66b (Figure 1A). Although the frequencies of circulating $CD326^+$ EC were higher in a fraction of HIV^+ participants *versus* HIV^-, differences did not reach statistical significance (Figure 1B; p=0.0733). Also, among TPV^+ participants, there was no correlation between the

frequency of CD326$^+$ EC and TPV neither in HIV$^+$ nor HIV$^-$ participants (Figure 1C). Thus, the presence of circulating CD326$^+$ EC in the blood of a fraction of HIV$^+$ participants is not indicative of subclinical atherosclerosis, but rather may reflect the epithelial barrier dysfunction and/or other oncologic/autoimmune events to be investigated.

Increased frequencies of CD4$^+$ T-cells expressing CD326 in HIV$^+$ *versus* HIV$^-$ participants

Our group previously reported alterations in CD4$^+$ T-cell phenotype and functions to be associated with the CVD status in ART-treated PWH [60, 68, 69]. To get more insights into these alterations, CD4$^+$ T-cells were immunophenotyped concerning their expression of TCRα/β and γ/δ heterodimers, activation molecules (i.e., CD69, HLA-DR), and gut-homing adhesion molecules (*i.e.*, Itgβ7, ItgαE) and chemokine receptors (*i.e.*, CCR6, CCR9) (Supplemental Figure 4). Our flow cytometry analysis brought our attention to the unexpected presence of a fraction of CD4$^+$ T-cells expressing the EC marker CD326 (Figure 2A), with CD326$^+$CD4$^+$ T-cells being more abundant in HIV$^+$ compared to HIV$^-$ participants (Figure 2B). Compared to total CD4$^+$ T-cells, the CD326$^+$CD4$^+$ subset of HIV$^+$ participants mostly expressed TCRαβ but distinguished from total CD4$^+$ T-cells by an increased expression of TCRγδ, CD69, HLA-DR, ItgαE, CCR6 and CCR9, and a decreased expression of Itgβ7 and Itgα4 (Supplemental Figure 5). The same phenotypic differences between total and CD326$^+$CD4$^+$ T-cells were also observed among HIV$^-$ participants (data not shown). Of particular interest, CD326$^+$CD4$^+$ T-cells of HIV$^+$ *versus* HIV$^-$ participants expressed at lower frequencies the TCRγδ, HLA-DR, ItgαE, and CCR9 but at higher frequency CD69, Itgβ7, and CCR6 (Figure 2C). Finally, the frequencies of CD326$^+$CD4$^+$ T-cells did not correlate with TPV neither among HIV$^+$ nor HIV$^-$ participants (Figure 2D). These results point to the presence in the circulation of HIV$^+$ *versus* HIV$^-$ participants of an atypical TCRαβ$^+$

$CD4^+$ T-cell population expressing the epithelial marker CD326, the activation marker CD69 and the gut homing markers Itgβ7 and CCR6, regardless of subclinical atherosclerosis.

Decreased frequencies of $CD8^+$ IELs in the peripheral blood of HIV^+ *versus* HIV^- participants

Another element of our hypothesis of observing gut immune alterations in peripheral blood was related to IELs. Using well-established markers in the literature [42-45, 70-72], we analyzed two subpopulations of IELs circulating in the blood: $CD8^+$ IELs ($CD3^+CD4^-$ $Itg\beta7^+ItgαE^+TCRαβ^+TCRγδ^-CD8αα^+CD8αβ^-$) and $CD4^+$ IELs ($CD3^+CD4^+Itg\beta7^+ItgαE^+TCRαβ^+TCRγδ^-CD8αβ^-$) (Supplemental Figures 1 and 6). Consistent with their expression of the gut-homing adhesion molecules Itgβ7 and ItgαE, we observed that $CD8^+$ and $CD4^+$ IELs distinguished from their respective total $CD8αβ^+$ and $CD4^+$ T-cell counterparts by superior levels of chemokine receptors CCR6 and CCR9, indicative of their imprinting for gut-homing (Supplemental Figure 7A-B). Further, our results show a decreased frequency of $CD8^+$ IELs in HIV^+ compared to HIV^- participants (Figure 3A), together with similar levels of CD69 and CCR6 but decreased CCR9 expression (Figure 3B). In contrast, the frequency of $CD4^+$ IELs was similar in HIV^+ compared to HIV^- participants (Figure 3C), and their expression of CD69 and CCR6 was equivalent in both groups, with CCR9 levels being reduced in HIV^+ participants (Figure 3D). The frequencies of $CD8αβ^+$ (Figure 3E) and $CD4^+$ IELs (Figure 3F) do not correlate with TPV in both HIV^+ and HIV^- groups. These results point to a deficit in circulating $CD8^+$ IELs in association with HIV status, a deficit that was not aggravated with subclinical atherosclerosis.

Increased frequencies of CCR6$^+$ItgB7$^-$ CD4$^+$ T-cells in the peripheral blood of HIV$^+$ *versus* HIV$^-$ participants, which correlate with subclinical atherosclerosis

Our group has previously reported that CCR6$^+$ CD4$^+$ T-cells exhibit increased permissiveness to HIV infection independently of Itgβ7 expression [33, 38]. Therefore, we investigated the frequency and phenotype (i.e., CD69, HLA-DR, ItgαE, and CCR9) of CD4$^+$ T-cells expressing or not CCR6 and/or Itgβ7 in our study participants (Supplemental Figure 8), in relationship with the HIV status and subclinical atherosclerosis (Figure 4). We found no significant differences in the frequency of CCR6$^+$Itgβ7$^+$ CD4$^+$ T-cells in HIV$^+$ compared to HIV$^-$ participants (Figure 4A). The expression of CD69, HLA-DR, and ItgαE on CCR6$^+$Itgβ7$^+$ CD4$^+$ T-cells was similar between HIV$^+$ and HIV$^-$ participants, with CCR9 expression being lower in HIV$^+$ participants (Figure 4B). Contrariwise, the frequency of CCR6$^+$Itgβ7$^-$ CD4$^+$ T-cells was higher in HIV$^+$ compared to HIV$^-$ participants (Figure 4C), and the expression of CD69 and HLA-DR was equivalent in both groups, with ItgαE and CCR9 expression levels being slightly lower in HIV$^+$ participants (Figure 4D). Of note, the expression of ItgαE and CCR9 was markedly lower in CCR6$^+$ItgB7$^-$ CD4$^+$ T-cells compared to the CCR6$^+$ItgB7$^+$ counterpart. Remarkably, the frequency of CCR6$^+$Itgβ7$^+$ (Figure 4E) and CCR6$^+$Itgβ7$^-$ CD4$^+$ T-cells (Figure 4F) correlated positively with TPV in HIV$^+$ but not HIV$^-$ participants, with the strongest capacity of CCR6$^+$Itgβ7$^-$ CD4$^+$ T-cells to predict TPV. These results point to a potential link between subclinical atherosclerosis and the frequency of CCR6$^+$Itgβ7$^+$ and especially CCR6$^+$Itgβ7$^-$ CD4$^+$ T-cell subsets, two subpopulations demonstrated by our group to have increased permissiveness to HIV-1 infection [38].

Multivariate analyses further confirm altered immune subpopulations in ART-treated PWH

To identify valuable HIV and CVD predictors, we performed a multivariate analysis of parameters that varied between our study participant groups (Supplemental File 1). The frequencies of all studied subpopulations can be found in Supplemental Table 1. Multivariate analyses related to HIV status and the presence of atherosclerotic plaque are detailed in Supplemental Tables 2 and 3, respectively.The basic logistic regression model, which only included the immune subsets (Crude Model), was evaluated against multivariate logistic regression models that adjusted for three different potential confounding factors (*i.e.*, BMI, TPV, LDL): all confounding factors together (Model 1), BMI (Model 2), TPV (Model 3), and LDL (Model 4), are detailed in Table 3. Across all models, the frequency of the following subpopulations was significantly associated with the HIV status: $CD4^+$ T-cells, $CD8^+$ T-cells, as well as the CD4/CD8 ratio, $CD326^+$ ECs, $CD326^+CD4^+$ T-cells, $CD326^+CD69^+$ $CD4^+$ T-cells, $CD326^+Itg\beta7^+$ $CD4^+$ T-cells, $CCR9^+CD4^+$ IELs, $CCR6^+Itg\beta7^-CD4^+$ T-cells, and $CCR6^+Itg\alpha E^+Itg\beta7^-CD4^+$ T-cells. A few subpopulations lost statistical significance with the HIV status when adjustments were made for cofounding factors $Itg\alpha E^+CD326^+CD4^+$ T-cells were no longer significantly associated on Models 1, 2 and 3; $TCR\gamma\delta^+CD326^+CD4^+$ T-cells lost their significance when adjusting for all parameters together (Model 1), but remained significant when adjusting for only one parameter; and, intriguingly, $CCR9^+CD8^+$ IELs gained statistical significance only on Models 1 and 2. Unfortunately, our multivariate analyses failed to predict subpopulations associated with CVD in the HIV^+ group in the raw model or upon univariate adjustment for smoking, D-dimer, and FRS (raw data in Supplemental Table 3). Nevertheless, we noted a minor tendency for statistical significance in predicting CVD among HIV^+

participants for $CD4^+$ T-cell counts (p=0.0749), CD4/CD8 ratio (p=0.0615), $CD326^+CD69^+CD4^+$ T-cells (p=0.1465) and $CD326^+Itg\alpha4^+CD4^+$ T-cells (p=0.1465) when adjusted for smoking, and for $CD8^+$ T-cell counts when adjusted for D-dimer (p=0.076). In summary, we identified circulating $CD326^+$ EC, specific CD4+ T-cell subsets (i.e., $CD326^+$, $CD326^+CD69^+$, $CD326^+Itg\beta7^+$, $CCR6^+Itg\beta7^-$, and $CCR6^+Itg\alpha E^+Itg\beta7^-$), and $CCR9^+CD4^+$ IELs as new markers associated with HIV status. These changes in circulating EC and immune cells potentially reflect intestinal barrier impairment in ART-treated PWH, with only a few of them being associated with subclinical atherosclerosis.

DISCUSSION

In this manuscript, we addressed the hypothesis that HIV-mediated alterations in gut barrier integrity could be detected in the peripheral blood of PWH and could be linked to the occurrence of subclinical CVD. This hypothesis was inspired by the concept of liquid biopsy used in oncology [52, 56, 57] and the evidence that inflammatory conditions in the intestines are associated with the unusual circulation in the blood of intestinal epithelial cells and other tissue-resident immune cells [53-55]. Our major findings point to ***i)*** aberrant circulation of $CD326^+$ EC, IEL, and $CD326^+CD4^+$ T-cells in the peripheral blood of HIV^+ *versus* HIV^- participants and ***ii)*** a positive association between TPV and the abundance of $CCR6^+CD4^+$ T-cells expressing or lacking the gut-homing marker Itgβ7, subsets previously identified by our group as being highly permissive to HIV infection [38]. These results are consistent with major intestinal barrier alterations during HIV-1 infection [12, 13, 24] and a documented link between the size of HIV reservoirs and subclinical CVD [73].

PBMCs from n=82 participants of the CHACS were analyzed, including 42 ART-treated PWH and 40 individuals without HIV. Both groups were further categorized according to whether they had atherosclerotic plaque or not. HIV^+ individuals in the TPV+ group showed significantly higher plaque volumes (median 851.7 mm^3) compared to their HIV^- counterparts (median 143 mm^3; $p<0.0001$), demonstrating an increased burden of coronary atherosclerosis despite similar levels of D-dimer, fibrinogen, HDL, and triglycerides between the groups. Notably, BMI and LDL levels were higher in the HIV^- group. Previous research involving other ART-treated CHACS participants also reported a higher incidence of atherosclerotic plaque in HIV^+ compared to the HIV^- group [60, 63]. The analysis of the HIV^+ group revealed that those with

plaque (TPV^+) had higher FRS and D-dimer compared to those without (TPV^-), further indicating a known link between these factors and cardiovascular events [74, 75]. Both TPV^+ and TPV^- groups showed similar duration of HIV infection, duration of ART, nadir CD4 counts, and current CD4 percentages, without association with TPV. Contrariwise, recent research conducted by our group, studying different patients from the same cohort, indicated a direct relationship between the duration of ART and the occurrence of atherosclerotic plaques [60]. In line with the HIV literature, our first analysis showed decreased $CD4^+$ T-cells and increased $CD8^+$ T-cells and an abnormal CD4/CD8 ratio in ART-treated PWH; however, these altered parameters showed no significant relation to the presence of atherosclerotic plaque. Interestingly, age and TPV correlated with the CD4/CD8 ratio in HIV^- but not in HIV^+ individuals, showing opposite trends between the two groups.

We originally observed a trend towards a higher frequency of EpCAM/$CD326^+$ ECs in the peripheral blood of PWH, in line with the documented gut barrier disruption during HIV infection [7, 12]. As CD326 plays a crucial role in establishing a functional intestinal barrier [48-50] and is a marker of circulating tumor cells in the context of liquid biopsies [50-52], investigating circulating and gut $CD326^+$ cells in larger cohorts could provide valuable insights into gut barrier integrity in HIV infection, to potentially become a patient-friendly approach to avoid invasive intestinal biopsies. To our knowledge, this is the first work to address circulating EpCAM/$CD326^+$ cells in HIV-1 infection, as previous studies employed this marker to remove epithelial cells of gut biopsy analyses [76, 77].

A noteworthy finding of our study was the existence and increased abundance of a subset of $CD4^+$ T-cells expressing the IEC marker CD326 in HIV^+ compared to HIV^- participants. Compared to the total $CD4^+$ T-cells of HIV^+ participants, $CD326^+CD4^+$ T-cells expressed an activated ($CD69^+HLA\text{-}DR^+$) and gut homing phenotype ($ItgαE^+CCR6^+CCR9^+$). A fraction of $CD326^+CD4^+$ T-cells also expressed TCRγδ although all cells expressed TCRαβ. Of note, unconventional T-cells that co-express unique markers, such as CD4, TCRαβ and TCRγδ, have been described before [78, 79]. Compared to HIV^-, $CD326^+CD4^+$ T-cells were significantly more abundant in HIV^+ participants. They displayed decreased expression of TCRγδ and higher expression of CD69 and CCR6. Like Th17 cells, TCRγδ T-cells are crucial for maintaining the gut barrier integrity [72] and are significantly perturbed during HIV-1 infection, even during effective ART, due to their expression of CD4, CCR5 and α4β7 [80-82].

The observation of lower TCRγδ expression can be an indicator of compromised gut immunity. CD69, an early activation marker of T-cells and a promotor of T-cell retention in tissues, is scarcely found in the circulation [83-85]. Our results demonstrate that these unconventional $CD326^+CD4^+$ T-cells are more activated in PWH, further associating the presence of the CD69 marker with T-cell activation in HIV-1 infection [86-88]. We have also observed increased CCR6 expression in $CD326^+CD4^+$ T-cells in this study. Previous research indicated that CCR6-expressing T-cells are more susceptible to HIV-1 [33, 39, 89, 90]. Untreated individuals show a higher amount of integrated HIV-DNA in $CCR6^+$ T-cells, and a higher count of these cells correlates with active viral replication [33, 39, 91-93]. While memory T-cells expressing both integrin α4β7 and CCR6 are inclined towards a Th17 lineage and are more vulnerable to HIV, it is primarily the expression of CCR6, rather than integrin α4β7 that reflects this susceptibility [38,

90, 93]. This underscores the critical role of CCR6 in mucosal inflammation and the progression of HIV infection.

By comparing the phenotype of the $CD326^{+}CD4^{+}$ T-cells to total conventional $CD4^{+}$ T-cells within HIV^{+} participants, we observed lower levels of the integrin subunits α4 and β7 but increased expression of αE/CD103, a hallmark of gut residency, specially when associated with CD69. The interaction between CD103 on T-cells and E-cadherin on IEC promotes the attachment and retention of T-cells within the intestinal epithelium [42, 94]. Both CD4 and CD8 cells expressing CD103 and CD69 are affected by HIV-1 [13, 46, 94, 95]. Moreover, $CD326^{+}CD4^{+}$ T-cells from HIV^{+} individuals were characterized by heightened expression of both CCR6 and CCR9 in comparison to conventional $CD4^{+}$ T-cells. HIV-1 exploits the gut-homing mechanism of CCR9 to target T-cells for infection, leading to a significant loss of these cells in the gut, which further contributes to the disruption of gut mucosal integrity [13, 41, 95]. Of note, CCR9 is associated with inflammatory conditions and its knockdown can reduce CVD progression [96].

Considering the unusual expression of the EC marker CD326 on $CD4^{+}$ T-cells, one may consider $CD326^{+}$ T-cells as cells with a mucosal-homing potential that might acquire CD326 expression through trogocytosis upon interaction with EC. Trogocytosis involves the transfer of surface molecules and membrane fragments from one cell to another, thereby granting recipient cells new functionalities or the ability to eliminate donor cells [97, 98]. Such mechanism has been reported in the context of HIV-1 infection [99, 100] and may reflect the history of cell-to-cell interactions *in vivo*.

Our investigations also found a reduced frequency of $CD8^+$ IELs in ART-treated PWH compared to HIV^- counterparts. The cell phenotype was characterized by TCRαβ and CD8αα expression, which reveal that they are "natural" IELs, distinct from "induced" IELs that primarily express CD4 or CD8αβ and derive from conventional $TCR\alpha\beta^+$ T-cells of peripheral lymphoid tissues. Natural IELs originate from precursor cells that have undergone development in the thymus and can migrate to the intestinal epithelium without the need for a cognate antigen [42, 43, 70]. Initially discovered in mice, the presence of $TCR\alpha\beta^+CD8\alpha\alpha^+$ IELs in humans is still debatable [70], although a low frequency (<1%) is documented in humans [43]. While their $TCR\alpha\beta^+CD8\alpha\beta^+$ and $TCR\gamma\delta^+CD8\alpha\alpha^+$ counterparts perform distinct functions within the immune system, $TCR\alpha\beta^+CD8\alpha\alpha^+$ IELs are particularly noted for their potential suppressive/regulatory contributions, as well as similarities with NK cells [43, 70].

Due to the lack of description of these IELs in human studies, research into their role in HIV infection is limited. Studies reported a significant reduction in the population of both $CD4^+$ and $CD4^+CD8\alpha\alpha^+$ IELs within the intestinal epithelium during the SIV/HIV infection [101, 102]. Other research mentions alterations in subsets that simultaneously expressed CD8αα and αβ [103]. Notably, in this work, the subset we examined did not exhibit co-expression of these markers. Therefore, to our knowledge, this is the first study documenting the diminution of $TCR\alpha\beta^+CD8\alpha\alpha^+$ IELs in the peripheral blood of PWH. Since IELs are key in targeting virus-infected IECs, via perforin, granzyme B, and IFN-γ and can perform CTL functions and secrete a broad spectrum of interferons, including types I, II, and III, supporting the antiviral state of the epithelium [71, 104], we speculate that their reduced frequency is associated with impaired

antiviral responses during HIV infection. $CD4^+$ IELs did not differ between HIV^+ and HIV^- groups in this study.

An interesting finding was that the presence of $CCR6^+Itg\beta7^-$ $CD4^+$ T-cells was augmented in HIV^+ individuals and strongly correlated with subclinical atherosclerosis. A minor association was also found for $CCR6^+Itg\beta7^+CD4^+$T-cells. This indicates a connection of the CCR6 receptor with CVD risk in PWH, in line with what was reported before in people without HIV with hypertension and CVD [105]. Our group and others have previously reported that CCR6 expression is a marker of HIV reservoirs [39, 91, 92]. Other research documented the presence of $CD4^+CD103^+CD69^+CCR6^{low}$ T-cells in the gut of PWH harboring HIV-DNA [46, 47]. This makes us further believe that the altered cells found in this work could represent HIV reservoirs, a hypothesis to be examined.

Finally, multivariate analyses identified new cell subsets as being disturbed in frequency, as well as activation and gut-homing in HIV^+ *versus* HIV^- and explored predictors of HIV and CVD status above other confounding well-established predictors. Interestingly, in this assessment, the frequency of $CD326^+$ IECs in PWH was significantly increased compared to HIV^- individuals, across all adjustment models. It corroborated the increase of $CCR6^+Itg\beta7^-CD4^+$ T-cells and unconventional $CD326^+CD4^+$ T-cells in PWH, which displayed higher CD69 and/or Itgβ7 expression. This analysis demonstrated the decrease of immune cell subpopulations in PWH, such as $TCR\gamma\delta^+CD326^+CD4^+$ T-cells, $CCR9^+CD4^+$ IELs, and $Itg\alpha E^+CCR6^+Itg\beta7^-CD4^+$ T-cells. One of the objectives of our study was to identify subpopulations associated with CVD during HIV infection, a goal that our multivariate analyses undesirably did not achieve, likely due to limitations in sample size. Nevertheless, disturbance in some subsets showed a tendency for

significant association with TPV in multivariate analysis when adjusted for smoking: CD4 counts, CD4/CD8 ratios, as well as $CD326^{+}CD69^{+}$ and $CD326^{+}Itg\alpha4^{+}CD4^{+}$ T-cells. Therefore, new studies will need to include larger study populations, focusing on these specific, unusual $CD4^{+}$ T-cells expressing the epithelial cell-specific marker CD326/EpCAM.

Altogether, our results support the idea that HIV-specific gut-immune axis alterations are mirrored in the peripheral blood of ART-treated PWH. These dysregulations comprised overt cell activation and odd cell phenotypes with gut-homing potential. The increased prevalence of unconventional $CD326^{+}CD4^{+}$ T-cells and decreased numbers of natural $CD8^{+}$ IELs in the peripheral blood suggest ongoing gut barrier disruption, which may predispose ART-treated PWH to increased CVD risk [6, 12, 18, 20, 21]. This study also identified a specific immune cell phenotype, $CCR6^{+}Itg\beta7^{-}CD4^{+}$ T-cells, associated with increased atherosclerotic plaque burden in PWH, linking these cellular alterations directly to CVD risk. Our results provide a compelling rationale for further investigation into targeted interventions that address not just viral suppression but also the unique immune mucosal dysregulation in ART-treated PWH, reflected in the peripheral blood, for reducing the CVD onset and mortality and improving long-term health outcomes in an aging PLW community.

COMPETING INTERESTS

The authors declare no financial and non-financial competing interests.

AUTHORS' CONTRIBUTIONS

EMG performed the experiments, analyzed the results, prepared the figures, and wrote the manuscript. JD helped with PBMC processing for flow cytometry analysis. REC helped with color compensation in Symphony. TWS generated preliminary data on circulating $CD326^+$ IECs. MN provided expertise with IELs. CC-L acquired and interpreted the cardiovascular imaging data. AF-M performed the multivariate statistical analysis. MEF, MD and CT provided protocols, access to human samples, and expertise with CVD. J-PR provided access to human samples. PA designed the study, analyzed the results, designed the figures, and revised the manuscript. All authors revised and approved the manuscript.

FUNDING

This work was supported in part by funds from the Canadian Institutes of Health Research (CIHR; PJT-153052; PJT-178127 to P.A.), National Institutes of Health (NIH) to CT and PA (R01AG054324), as well as infrastructure funding from the Canadian Foundation for Innovation (CFI) to PA and CT. Core facilities and human cohorts were supported by the *Fondation du CHUM* and the *Fonds de recherche du Québec – Santé* (FRQ-S) HIV/AIDS and Infectious Diseases Network. MD receives a clinician-researcher salary award from the *Fonds de recherche du Québec – Santé*. The CHACS cohort is supported by funds from CIHR (HAL 398643 to MD) and by the CHIR HIV clinical trial network (CTN-272). The funding institutions played no role in the design, collection, analysis, and interpretation of data.

ACKNOWLEDGEMENTS

The authors thank Philippe St-Onge and Gael Dulude (Flow Cytometry Core Facility, CHUM-Research Centre) for expert technical support with polychromatic flow cytometry sorting; Olfa Debbeche for managing the NLC3 Core Facility of the CHUM-Research Centre; Dr. Annie Chamberland, Stéphanie Matte, Mohamed Sylla for blood processing and managing the cell biobank; Marc Messier-Peet for providing clinical information and managing the CHACS database; and Mario Legault for his help with ethical approvals and informed consents. The authors address a special thanks to all study participants for their crucial contribution to this work.

FIGURE LEGENDS

Figure 1: Frequency of peripheral blood CD326$^+$ IEC in HIV$^+$ *versus* HIV$^-$ participants relative to subclinical CVD. PBMCs from HIV$^+$ART (n=22) and HIV$^-$ (n=20) participants with known CVD status measured as the total plaque volume (TPV; mm^3) of the coronary artery atherosclerosis were stained with the epithelial cell marker CD326/EpCAM and a cocktail of cell lineage abs recognizing various subsets of immune cells, as follows CD45, CD3, CD4, CD69, HLA-DR, TCRαβ, TCRγδ, CD8αβ CD8αα, CD49d/Integrin(Itg)α4, Itgβ7, CD103/ItgαE, CD196/CCR6, CD199/CCR9. The Fixable Viability Stain 575V was used to exclude dead cells from the analysis. Cell frequencies and phenotypes were analyzed by flow cytometry (BD Fortessa and FlowJo). Non-immune CD45$^-$ cells were gated as in Supplemental Figure 1 and circulating intestinal epithelial cells (IEC) were identified as cells with a CD45$^-$CD326$^+$ phenotype. Shown are **(A)** the flow cytometry gating strategy to identify the presence of CD326$^+$ IECs in PBMCs; **(B)** the frequency (%) of circulating CD326$^+$ IEC in HIV$^+$ *versus* HIV$^-$ participants, and **(C)** the % of CD326$^+$ IEC in relationship to HIV status in PBMCs of study participants; and the correlation between TPV and the % of CD326$^+$ IECs in PBMCs of HIV$^+$ and HIV$^-$ participants, respectively. Mann-Whitney p-values (one-tailed) **(B)**, as well as Spearman correlation p and r values **(C)**, are indicated on the graphs.

Figure 2: Frequency and phenotype of peripheral blood CD326$^+$ CD4$^+$ T-cells in HIV$^+$ *versus* HIV$^-$ participants relative to subclinical CVD. PBMCs from study participants were identified as per Supplemental Figure 1. Shown are the representative gating **(A)** and the frequency **(B)** of circulating CD326$^+$ CD4$^+$ T-cells in HIV$^+$ *versus* HIV$^-$ participants; **(C)** the phenotypical characterization of CD326$^+$ CD4$^+$ T-cells in terms of expression of TCR (αβ and

γδ), activation molecules (CD69 and HLA-DR), integrins (Itgβ7 and ItgαE) and gut-homing receptors (CCR6 and CCR9) of circulating CD326$^+$ CD4$^+$ of HIV$^+$ *versus* HIV$^-$ participants; and **(D)** the correlation between the frequency of CD326$^+$ CD4+ T-cells and TPV in HIV$^+$ **(left panel)** and HIV$^-$ **(right panel)** participants. Mann-Whitney p-values **(B-C)**, as well as Spearman correlation p and r values **(D)**, are indicated on the graphs.

Figure 3: Frequency and phenotype of peripheral blood CD8+ and CD4+ IEL in HIV+ *versus* HIV- participants relative to subclinical CVD. (A-F) PBMCs from HIV+ART (n=22) and HIV- (n=20) participants with known CVD status measured as the TPV (mm^3) of the coronary artery atherosclerosis were stained with t a cocktail of cell lineage abs (CD45, CD3, CD4, CD69, HLA-DR, TCRαβ, TCRγδ, CD8αβ CD8αα, CD49d/Integrin(Itg)α4, Itgβ7, CD103/ItgαE, CD196/CCR6, CD199/CCR9). The Fixable Viability Stain 575V was used to exclude dead cells from the analyses. Cell frequencies and phenotypes were analyzed by flow cytometry (BD Fortessa and FlowJo). Shown are the frequency of circulating CD8$^+$ **(A)** and CD4$^+$ **(C)** IELs in HIV$^+$ *versus* HIV$^-$ participants; and the characterization of the expression of TCRαβ, CD69, CCR6 and CCR9 on circulating CD8$^+$ **(B)** and CD4$^+$ **(D)** IELs in HIV$^+$ *versus* HIV$^-$ participants. Finally, shown is the correlation between TPV and the frequency of CD8$^+$ **(E)** and CD4$^+$ **(F)** IELs in HIV$^+$ **(left panels)** and HIV$^-$ **(right panels)** participants, respectively; and **(F)** the correlation between TPV and the frequency of CD4$^+$ IELs in HIV$^+$ and HIV$^-$ participants, respectively. Mann-Whitney p-values **(A-D)**, as well as Spearman correlation p and r values **(E-F)**, are indicated on the graphs.

Figure 4: Frequency and phenotype of peripheral blood CCR6$^+$CD4$^+$ T-cells expressing the gut-homing Itgβ7 in HIV$^+$ and HIV$^-$ participants relative to subclinical CVD. (A-F) PBMCs from HIV$^+$ART (n=22) and HIV$^-$ (n=20) participants with known CVD status measured as the TPV (mm^3) of the coronary artery atherosclerosis were stained with a cocktail of cell lineage abs (CD45, CD3, CD4, CD69, HLA-DR, TCRαβ, TCRγδ, CD8αβ CD8αα, CD49d/Itgα4, Itgβ7, CD103/ItgαE, CD196/CCR6, CD199/CCR9). The fixable Viability Stain 575V was used to exclude dead cells from the analysis. Cell frequencies and phenotypes were analyzed by flow cytometry (BD Fortessa and FlowJo). Shown are the frequencies of circulating CD4$^+$ T-cells with a CCR6$^+$Itgβ7$^+$ **(A)** and CCR6$^+$Itgβ7$^-$ **(C)** phenotypes in HIV$^+$ *versus* HIV$^-$ participants; and the characterization of the expression of CD69, HLA-DR, ItgαE, and CCR9, on circulating CCR6$^+$Itgβ7$^+$ **(B)** and CCR6$^+$Itgβ7$^-$ **(D)** CD4$^+$ T-cells in HIV$^+$ *versus* HIV$^-$ participants. Finally, shown is the correlation between TPV and the frequency of CCR6$^+$Itgβ7$^+$ **(E)** and CCR6$^+$Itgβ7$^-$ **(F)** CD4$^+$ T-cells in HIV$^+$ **(right panels)** and HIV$^-$ participants **(left panels)**. Mann-Whitney p-values **(A-D)**, as well as Spearman correlation p and r values **(E-F)**, are indicated on the graphs.

TABLES

Table 1: Description of study participants

	HIV$^+$ (n=42)	**HIV$^-$** (n=40)	**p-value**
Demographics and clinical information			
Age (years)*	54.2±5.48	54.6±8.34	0.832
Male&	40 (95%)	34 (85%)	0.150
BMI (kg/m2)#	24.62 (19.08-34.55)	27.22 (19.66-44.05)	**0.005**
Framingham Score#	9 (3-30)	10 (2-18)	0.339
Smoking& Never Current Smoker Former Smoker N/A	 11 (26%) 17 (41%) 13 (31%) 1 (2%)	 18 (45%) 10 (25%) 12 (30%) 0 (0%)	0.212
Statin treatment&	18 (43%)	6 (15%)	**0.007**
Coronary Artery Disease Parameters			
Total Plaque Volume (mm^3)#	851.7 (425.2-1981) n=21	143 (34-2253) n=20	**<0.0001**
Laboratory Parameters			
D-Dimer (μg/L)#	353.5 (170- 1130)	327.3 (170- 580)	0.683
Fibrinogen (G/L)#	3.26 (2.09- 6.10)	2.92 (2.14- 4.21)	0.453
LDL (mmol/L)#	2.75 (0.82-4.55)	3.2 (1.61-6.9)	**0.046**
HDL (mmol/L)#	1.23 (0.77-2.2)	1.31 (0.73-1.92)	0.174
Triglycerides (mmol/L)#	1.87 (0.62-6.50)	1.60 (0.61-6.40)	0.214

*, for numeric parametric variables: mean±SD and t-Test were used; #for numeric non-parametric variables: median, interquartile range (IQR), and Mann-Whitney test were used. &, Categorical variables were compared with Fisher's Exact test (2 categories) and Chi-square (3 categories).

Table 2: Clinical parameters of ART-treated PWH with and without atherosclerosis

	TPV+ (n=21)	TPV- (n= 21)	p-value
Demographics and clinical information			
Age (years)*	54.8±5.05	53.7±5.95	0.515
Male&	21 (100%)	19 (90.5%)	0.488
BMI (kg/m2)#	24 (19-34.5)	25.4 (21-31.6)	0.057
Framingham Score#	12.2 (5-30)	8.5 (3-18)	**0.039**
Smoking& Never Smoked Current Smoker Former Smoker N/A	 1 (5%) 14 (66%) 6 (29%) 0 (0%)	 10 (48%) 3 (10%) 7 (33%) 1 (5%)	**0.001**
Statin treatment&	14 (67%)	4 (19%)	**0.004**
Laboratory Parameters			
D-Dimer (ug/L)#	373.5 (170- 720)	325.0 (170- 1130)	**0.049**
Fibrinogen (G/L)#	3.6 (2.09- 6.13)	2.8 (2.13- 3.7)	0.075
LDL (mmol/L)#	2.6 (0.82- 4.33)	2.9 (1.45- 4.55)	0.351
HDL (mmol/L)#	1.24 (0.77-2.04)	1.23 (0.82-2.04)	0.975
Triglycerides (mmol/L)#	2.29 (0.62-6.5)	1.45 (0.75- 3.23)	0.056
Serology			
Co-infection CMV#	18 (86%)	15 (71%)	0.194
HIV disease parameters			
Duration of HIV (years)*	20.3 (5.7-30.8)	17.5 (3.8-29.5)	0.236
Duration of ART (years)*	17.3±5.7	14±7.4	0.065
Nadir CD4 (xE9/L)#	240 (20- 576)	242 (10-750)	0.678
CD4 (%)	44% ±16.7	48% ±18.5	0.369

*, for numeric parametric variables: mean±SD and t-test were used; #for numeric non-parametric variables: median, interquartile range (IQR), and Mann-Whitney test were used. &, Categorical variables were compared with Fisher's Exact test (2 categories) and Chi-square (3 categories).

Table 3: Logistic regression prediction analysis for the association between HIV status and cell subsets in study participants

	Crude Model	Model 1	Model 2	Model 3	Model 4
	OR (CI) (Min-Max) Adj. p value				
CD4+ T cells	0.15 (0.06–0.34) **<0.001**	0.12 (0.04–0.34) **<0.001**	0.16 (0.07–0.38) **<0.001**	0.14 (0.06–0.35) **<0.001**	0.10 (0.04–0.30) **<0.001**
CD8+ T cells	2.27 (1.34–3.87) **0.002**	1.89 (1.04–3.41) **0.035**	1.85 (1.07–3.18) **0.027**	2.44 (1.36–4.37) **<0.001**	2.12 (1.24–3.64) **0.006**
CD4/CD8 ratio	0.19 (0.09–0.42) **<0.001**	0.21 (0.09–0.48) **<0.001**	0.23 (0.10–0.50) **<0.001**	2.44 (1.37–4.37) **0.002**	0.19 (0.08–0.43) **<0.001**
CD326+ EC	3.58 (1.26–10.1) **0.016**	7.10 (1.34–37.6) **0.022**	4.87 (1.31–18.1) **0.018**	4.12 (1.30–13.1) **0.016**	3.57 (1.23–10.3) **0.019**
CD326+ CD4+ T-cells	6.62 (2.1–20.9) **0.004**	7.18 (1.85–27.8) **0.022**	6.71 (1.92–23.3) **0.014**	6.75 (2.01–22.6) **0.006**	5.71 (1.80–18.2) **0.010**
TCRγδ+CD326+ CD4+ T-cells	0.42 (0.24–0.71) **0.004**	0.53 (0.30–0.94) 0.062	0.49 (0.28–0.84) **0.036**	0.41 (0.24–0.72) **0.006**	0.44 (0.25–0.75) **0.010**
CD69+CD326+ CD4+ T-cells	7.55 (2.35–24.3) **0.004**	14.0 (2.92–67.5) **0.009**	10.7 (2.68–43.0) **0.007**	7.15 (2.19–23.3) **0.006**	9.84 (2.53–38.2) **0.009**
Itgβ7+CD326+ CD4+ T-cells	2.08 (1.19–3.63) **0.025**	2.35 (1.18–4.68) **0.049**	2.14 (1.16–3.92) **0.035**	2.02 (1.14–3.60) **0.040**	2.22 (1.20–4.07) **0.015**
ItgαE+CD326+ CD4+ T-cells	1.76 (1.08–2.88) **0.004**	1.96 (1.07–3.58) 0.062	1.78 (1.05–3.03) 0.065	1.72 (1.04–2.85) 0.069	1.98 (1.16–3.38) **0.025**
CCR9+CD8+ IELs	0.55 (0.34–0.89) 0.064	0.43 (0.24–0.77) **0.026**	0.49 (0.91–2.68) **0.004**	1.76 (1.04–2.30) 0.065	0.55 (0.34–0.90) 0.053
CCR9+CD4+ IELs	0.24 (0.11–0.51) **0.001**	0.27 (0.12–0.60) **0.008**	0.26 (0.12–0.57) **0.004**	0.24 (0.11–0.51) **0.001**	0.25 (0.11–0.55) **0.003**
CCR6+Itgβ7- CD4+ T-cells	3.35 (1.77–6.34)	3.98 (1.78–8.87)	4.38 (2.00–9.57)	3.08 (1.60–6.00)	3.45 (1.75–6.81)

	0.002	**0.007**	**0.002**	**0.007**	**0.003**
ItgαE +CCR6+ Itgβ7- CD4+ T-cells	0.40 (0.23–0.71) **0.009**	0.45 (0.24–0.84) 0.060	0.39 (0.21–0.73) **0.015**	0.41 (0.23–0.74) **0.017**	0.42 (0.23–0.74) **0.015**

OR, odds ratio; CI, 95% confidence interval; Adj. p, adjusted p-values.
Crude Model: no adjustment
Model 1: adjustment for BMI, TPV, and LDL
Model 2: adjustment for BMI
Model 3: adjustment for TPV
Model 4: adjustment for LDL

SUPPLEMENTAL FIGURE LEGENDS

Supplemental Figure 1 (related to Figure 1): General gating strategy for flow cytometry analysis of PBMCs of study participants. PBMCs from HIV$^+$ART (n=22) and HIV$^-$ (n=20) participants with known CVD status, measured as the total plaque volume (TPV; mm^3) of the coronary artery atherosclerosis, were stained with the Fixable Viability Stain 575V for dead cell exclusion and with a cocktail of abs that allowed the exclusion of other lineage cells (CD33, CD56, CD19 and CD66b), and the identification of CD45$^+$ hematopoietic cells. Among CD45$^+$ cells, CD3$^+$ T-cells were further differentiated into CD4$^+$ and CD8αβ$^+$ T-cells.

Supplemental Figure 2 (related to Figure 1): Frequency of CD4+ and CD8+ T-cells in HIV+ *versus* HIV- participants relative to age and subclinical CVD. PBMCs from study participants were identified as per Supplemental Figure 1. Shown are **(A)** the frequency of CD4$^+$ T-cells, CD8$^+$ T-cells and the CD4/CD8 ratio relative to the HIV status; **(B)** the characterization of CD4$^+$ T-cells, CD8$^+$ T-cells and CD4/CD8 ratio relative to the presence of subclinical CVD; **(C)** the correlation between age and the CD4/CD8 ratio in HIV$^+$ **(left panel)** and HIV$^-$ **(right panel)** participants; and **(D)** the correlation between TPV and the CD4/CD8 ratio in HIV$^+$ **(left panel)** and HIV$^-$ **(right panel)** participants. Mann-Whitney p-values, as well as Spearman correlation p and r values, are indicated on the graphs.

Supplemental Figure 3 (related to Figure 1): Preliminary data on the frequency of peripheral blood CD326+ EC in HIV$^+$ *versus* HIV$^-$ individuals. PBMCs from HIV$^+$ART (n=16) and HIV$^-$ (n=5) individuals were stained with the epithelial cell marker CD326/EpCAM and a cocktail of cell lineage abs recognizing various subsets of immune cells, as CD45, CD3,

CD4. The LIVE/DEAD™ Fixable Aqua Dead Cell Stain was used to exclude dead cells from the analysis. Cell frequencies and phenotypes were analyzed by flow cytometry (BD LSR II and FlowJo). Non-immune $CD45^-$ cells were gated within live cells and circulating epithelial cells (EC) were identified as cells with a $CD45^-CD326^+$ phenotype. Shown is the frequency (%) of circulating $CD326^+$ EC in HIV^+ *versus* HIV^- individuals.

Supplemental Figure 4 (related to Figure 2): Identification and phenotypic characterization of $CD326^+$ $CD4^+$ T-cells in PBMCs of HIV^+ and HIV^- study participants. PBMCs from study participants were identified as per Supplemental Figure 1. Shown is the analysis of the expression of TCRαβ, TCRγδ, CD69, HLA-DR, Itgβ7, ItgαE, CCR6, and CCR9 in cells from HIV^+ study participants.

Supplemental Figure 5 (related to Figure 2): Phenotype of $CD326^+$ *versus* total $CD4^+$ T in HIV^+ study participants. PBMCs from study participants were identified as per Supplemental Figure 1 and phenotypically analyzed as in Supplemental Figure 4. Shown is the phenotypical characterization of the expression of TCR (αβ and γδ), activation molecules (CD69 and HLA-DR), gut-homing integrins (Itgβ7, Itgα4 and ItgαE) and chemokine receptors (CCR6 and CCR9) in circulating $CD326^+$ *versus* total $CD4^+$ T-cells in HIV^+ study participants.

Supplemental Figure 6 (related to Figure 3): Flow cytometry gating strategy to identify $CD8^+$ and $CD4^+$ IELs in PBMCs. PBMCs from study participants were identified as per Supplemental Figure 1. Shown are the gating strategy for the identification of **(A)** CD8+ IELs as $CD3^+CD4^-$ T-cells co-expressing Itgβ7 and ItgαE relative to the expression of TCRαβ, or

TCRγδ, and CD8αβ or CD8αα; and **(B)** $CD4^+$ IELs as $CD3^+CD4^+$ T-cells co-expressing Itgβ7 and ItgαE relative to the expression of TCRαβ, or TCRγδ.

Supplemental Figure 7 (related to Figure 3): Phenotype of Total T-cells *versus* IELs in study participants. PBMCs from study participants were identified as per Supplemental Figure 1 and phenotypically analyzed as in Supplemental Figure 3. Shown is the phenotypical characterization of the expression of chemokine receptors (CCR6 and CCR9) in total circulating $CD8^+$ T-cells *versus* $CD8^+$ IELs **(A)** and Total $CD4^+$ T-cells *versus* $CD4^+$ IELs **(B)** in study participants.

Supplemental Figure 8 (related to Figure 4): Flow cytometry gating strategy to analyze the presence and phenotype of $CCR6^+$ $CD4^+$ T-cells co-expressing or not the gut-homing Itgβ7 in PBMCs of HIV^+ and HIV^- study participants. PBMCs from study participants were identified as per Supplemental Figure 1. Shown are the gating for the identification of $CD3^+CD4^+$ T-cells **(A)** expressing CCR6 and/or Itgβ7 **(B)** in PBMCs of HIV^+ **(left panels)** and HIV^- **(right panels)** participants; and the **(C)** analysis of the expression of CD69, HLA-DR, ItgαE, CCR9 in $CCR6^+CD4^+$ T-cells expressing or not Itgβ7 in PBMCs of HIV^+ study participants.

REFERENCES

1. WHO. *HIV data and statistics*. 2023 [cited 2023 Nov 11]; Available from: https://www.who.int/teams/global-hiv-hepatitis-and-stis-programmes/hiv/strategic-information/hiv-data-and-statistics.
2. Barre-Sinoussi, F., A.L. Ross, and J.F. Delfraissy, *Past, present and future: 30 years of HIV research*. Nat Rev Microbiol, 2013. **11**(12): p. 877-83.
3. Deeks, S.G., et al., *Research priorities for an HIV cure: International AIDS Society Global Scientific Strategy 2021*. Nat Med, 2021. **27**(12): p. 2085-2098.
4. Zicari, S., et al., *Immune Activation, Inflammation, and Non-AIDS Co-Morbidities in HIV-Infected Patients under Long-Term ART*. Viruses, 2019. **11**(3).
5. Akusjarvi, S.S. and U. Neogi, *Biological Aging in People Living with HIV on Successful Antiretroviral Therapy: Do They Age Faster?* Curr HIV/AIDS Rep, 2023. **20**(2): p. 42-50.
6. Perkins, M.V., et al., *Cardiovascular Disease and Thrombosis in HIV Infection*. Arterioscler Thromb Vasc Biol, 2023. **43**(2): p. 175-191.
7. Mudd, J.C. and J.M. Brenchley, *Gut Mucosal Barrier Dysfunction, Microbial Dysbiosis, and Their Role in HIV-1 Disease Progression*. J Infect Dis, 2016. **214 Suppl 2**: p. S58-66.
8. Agrati, C., et al., *The importance of advanced cytometry in defining new immune cell types and functions relevant for the immunopathogenesis of HIV infection*. AIDS, 2020. **34**(15): p. 2169-2185.
9. Paiardini, M. and M. Muller-Trutwin, *HIV-associated chronic immune activation*. Immunol Rev, 2013. **254**(1): p. 78-101.

10. Rousseau, R.K., et al., *Activation and gut-homing of peripheral T cells in HIV immunologic non-responders despite long term viral suppression.* PLoS One, 2021. **16**(7): p. e0254149.

11. Brenchley, J.M. and D.C. Douek, *Microbial translocation across the GI tract.* Annu Rev Immunol, 2012. **30**: p. 149-73.

12. Moretti, S., et al., *HIV-1-Host Interaction in Gut-Associated Lymphoid Tissue (GALT): Effects on Local Environment and Comorbidities.* Int J Mol Sci, 2023. **24**(15).

13. Veazey, R.S., *Intestinal CD4 Depletion in HIV / SIV Infection.* Curr Immunol Rev, 2019. **15**(1): p. 76-91.

14. McBride, J.A. and R. Striker, *Imbalance in the game of T cells: What can the CD4/CD8 T-cell ratio tell us about HIV and health?* PLoS Pathog, 2017. **13**(11): p. e1006624.

15. Lu, W., et al., *CD4:CD8 ratio as a frontier marker for clinical outcome, immune dysfunction and viral reservoir size in virologically suppressed HIV-positive patients.* J Int AIDS Soc, 2015. **18**(1): p. 20052.

16. Grossman, Z., et al., *Pathogenesis of HIV infection: what the virus spares is as important as what it destroys.* Nat Med, 2006. **12**(3): p. 289-95.

17. Thompson, C.G., C.L. Gay, and A.D.M. Kashuba, *HIV Persistence in Gut-Associated Lymphoid Tissues: Pharmacological Challenges and Opportunities.* AIDS Res Hum Retroviruses, 2017. **33**(6): p. 513-523.

18. Epple, H.J. and M. Zeitz, *HIV infection and the intestinal mucosal barrier.* Ann N Y Acad Sci, 2012. **1258**: p. 19-24.

19. El-Far, M. and C.L. Tremblay, *Gut microbial diversity in HIV infection post combined antiretroviral therapy: a key target for prevention of cardiovascular disease.* Curr Opin HIV AIDS, 2018. **13**(1): p. 38-44.

20. So-Armah, K., et al., *HIV and cardiovascular disease.* Lancet HIV, 2020. **7**(4): p. e279-e293.

21. Lewis, C.V. and W.R. Taylor, *Intestinal barrier dysfunction as a therapeutic target for cardiovascular disease.* Am J Physiol Heart Circ Physiol, 2020. **319**(6): p. H1227-H1233.

22. Guenin-Mace, L., P. Konieczny, and S. Naik, *Immune-Epithelial Cross Talk in Regeneration and Repair.* Annu Rev Immunol, 2022.

23. Mahapatro, M., L. Erkert, and C. Becker, *Cytokine-Mediated Crosstalk between Immune Cells and Epithelial Cells in the Gut.* Cells, 2021. **10**(1).

24. Wacleche, V.S., et al., *The Th17 Lineage: From Barrier Surfaces Homeostasis to Autoimmunity, Cancer, and HIV-1 Pathogenesis.* Viruses, 2017. **9**(10).

25. Buckner, J.H. and O.J. Harrison, *Th17 cells: from gut homeostasis to CNS pathogenesis.* Trends Immunol, 2022. **43**(3): p. 167-169.

26. Kim, C.J., et al., *Mucosal Th17 cell function is altered during HIV infection and is an independent predictor of systemic immune activation.* J Immunol, 2013. **191**(5): p. 2164-73.

27. Arthos, J., et al., *The Role of Integrin alpha(4)beta(7) in HIV Pathogenesis and Treatment*. Curr HIV/AIDS Rep, 2018. **15**(2): p. 127-135.

28. Pollock, J. and R. Kaul, *How integral is the alpha4beta7 integrin to HIV transmission?* EBioMedicine, 2021. **63**: p. 103148.

29. Wang, S., et al., *Distinct chemokines selectively induce HIV-1 gp120-integrin alpha4beta7 binding via triggering conformer-specific activation of alpha4beta7.* Signal Transduct Target Ther, 2021. **6**(1): p. 265.

30. Wang, X., et al., *Monitoring alpha4beta7 integrin expression on circulating CD4+ T cells as a surrogate marker for tracking intestinal CD4+ T-cell loss in SIV infection.* Mucosal Immunol, 2009. **2**(6): p. 518-26.

31. Sivro, A., et al., *Integrin alpha(4)beta(7) expression on peripheral blood CD4(+) T cells predicts HIV acquisition and disease progression outcomes.* Sci Transl Med, 2018. **10**(425).

32. Kader, M., et al., *Alpha4(+)beta7(hi)CD4(+) memory T cells harbor most Th-17 cells and are preferentially infected during acute SIV infection.* Mucosal Immunol, 2009. **2**(5): p. 439-49.

33. Gosselin, A., et al., *Peripheral blood CCR4+CCR6+ and CXCR3+CCR6+CD4+ T cells are highly permissive to HIV-1 infection.* J Immunol, 2010. **184**(3): p. 1604-16.

34. Planas, D., et al., *HIV-1 selectively targets gut-homing CCR6+CD4+ T cells via mTOR-dependent mechanisms.* JCI Insight, 2017. **2**(15).

35. Wacleche, V.S., et al., *The colocalization potential of HIV-specific CD8+ and CD4+ T-cells is mediated by integrin beta7 but not CCR6 and regulated by retinoic acid.* PLoS One, 2012. **7**(3): p. e32964.

36. Cicala, C., et al., *The integrin alpha4beta7 forms a complex with cell-surface CD4 and defines a T-cell subset that is highly susceptible to infection by HIV-1.* Proc Natl Acad Sci U S A, 2009. **106**(49): p. 20877-82.

37. Lu, X., et al., *Preferential loss of gut-homing alpha4beta7 CD4(+) T cells and their circulating functional subsets in acute HIV-1 infection.* Cell Mol Immunol, 2016. **13**(6): p. 776-784.

38. Monteiro, P., et al., *Memory CCR6+CD4+ T cells are preferential targets for productive HIV type 1 infection regardless of their expression of integrin beta7.* J Immunol, 2011. **186**(8): p. 4618-30.

39. Renault, C., et al., *Th17 CD4+ T-Cell as a Preferential Target for HIV Reservoirs.* Front Immunol, 2022. **13**: p. 822576.

40. Fert, A., et al., *Targeting Th17 cells in HIV-1 remission/cure interventions.* Trends Immunol, 2022. **43**(7): p. 580-594.

41. Mavigner, M., et al., *Altered CD4+ T cell homing to the gut impairs mucosal immune reconstitution in treated HIV-infected individuals.* J Clin Invest, 2012. **122**(1): p. 62-9.

42. Sumida, H., *Dynamics and clinical significance of intestinal intraepithelial lymphocytes.* Immunol Med, 2019. **42**(3): p. 117-123.

43. Van Kaer, L. and D. Olivares-Villagomez, *Development, Homeostasis, and Functions of Intestinal Intraepithelial Lymphocytes.* J Immunol, 2018. **200**(7): p. 2235-2244.

44. Cheroutre, H., F. Lambolez, and D. Mucida, *The light and dark sides of intestinal intraepithelial lymphocytes.* Nat Rev Immunol, 2011. **11**(7): p. 445-56.

45. Lockhart, A., D. Mucida, and A.M. Bilate, *Intraepithelial Lymphocytes of the Intestine.* Annu Rev Immunol, 2024.

46. Kiniry, B.E., et al., *Detection of HIV-1-specific gastrointestinal tissue resident CD8(+) T-cells in chronic infection.* Mucosal Immunol, 2018. **11**(3): p. 909-920.

47. Yukl, S.A., et al., *Shared Mechanisms Govern HIV Transcriptional Suppression in Circulating CD103(+) and Gut CD4(+) T Cells.* J Virol, 2020. **95**(2).

48. Huang, L., et al., *Functions of EpCAM in physiological processes and diseases (Review).* Int J Mol Med, 2018. **42**(4): p. 1771-1785.

49. Lei, Z., et al., *EpCAM Is Essential to Maintaining the Immune Homeostasis of Intestines via Keeping the Expression of pIgR in the Intestinal Epithelium of Mice.* Front Immunol, 2022. **13**: p. 843378.

50. Yahyazadeh Mashhadi, S.M., et al., *Shedding light on the EpCAM: An overview.* J Cell Physiol, 2019. **234**(8): p. 12569-12580.

51. Lin, D., et al., *Circulating tumor cells: biology and clinical significance.* Signal Transduct Target Ther, 2021. **6**(1): p. 404.

52. Alix-Panabieres, C. and K. Pantel, *Liquid Biopsy: From Discovery to Clinical Application.* Cancer Discov, 2021. **11**(4): p. 858-873.

53. Hegazy, A.N., et al., *Circulating and Tissue-Resident CD4(+) T Cells With Reactivity to Intestinal Microbiota Are Abundant in Healthy Individuals and Function Is Altered During Inflammation.* Gastroenterology, 2017. **153**(5): p. 1320-1337 e16.

54. Samat, A.A.K., et al., *Tissue-Resident Memory T Cells in Chronic Inflammation-Local Cells with Systemic Effects?* Cells, 2021. **10**(2).

55. Asawa, S., et al., *Circulating tumour cells in gastrointestinal cancers: food for thought?* Br J Cancer, 2023. **128**(11): p. 1981-1990.

56. Han, D., et al., *Liquid biopsy for infectious diseases: a focus on microbial cell-free DNA sequencing.* Theranostics, 2020. **10**(12): p. 5501-5513.

57. Fu, Y., Y. Zhang, and B.L. Khoo, *Liquid biopsy technologies for hematological diseases.* Med Res Rev, 2021. **41**(1): p. 246-274.

58. Talotta, D., et al., *Liquid biopsy in hematological malignancies: current and future applications.* Front Oncol, 2023. **13**: p. 1164517.

59. Giguere, K., et al., *Baseline characteristics of a prospective cohort study of aging and cardiovascular diseases among people living with HIV.* HIV Med, 2023. **24**(12): p. 1210-1221.

60. Wiche Salinas, T.R., et al., *Alterations in Th17 Cells and Non-Classical Monocytes as a Signature of Subclinical Coronary Artery Atherosclerosis during ART-Treated HIV-1 Infection.* Cells, 2024. **13**(2).

61. Chen, Z., et al., *In vivo coronary artery plaque assessment with computed tomography angiography: is there an impact of iterative reconstruction on plaque volume and attenuation metrics?* Acta Radiol, 2017. **58**(6): p. 660-669.

62. Durand, M., et al., *The Canadian HIV and aging cohort study - determinants of increased risk of cardio-vascular diseases in HIV-infected individuals: rationale and study protocol.* BMC Infect Dis, 2017. **17**(1): p. 611.

63. Boldeanu, I., et al., *Prevalence and Characterization of Subclinical Coronary Atherosclerotic Plaque with CT among Individuals with HIV: Results from the Canadian HIV and Aging Cohort Study.* Radiology, 2021. **299**(3): p. 571-580.

64. RCoreTeam. *R: A language and environment for statistical computing. R Foundation for Statistical Computing, Vienna, Austria.* 2018; Available from: https://www.R-project.org/.

65. Schlesselman, J.J., *Case-Control Studies: Design, Conduct, Analysis*. 1982: Oxford University Press.

66. Kenward, M.G. and J.H. Roger, *The use of baseline covariates in crossover studies.* Biostatistics, 2010. **11**(1): p. 1-17.

67. Benjamini, Y. and Y. Hochberg, *Controlling the False Discovery Rate: A Practical and Powerful Approach to Multiple Testing.* Journal of the Royal Statistical Society: Series B (Methodological), 1995. **57**(1): p. 289-300.

68. Ramani, H., et al., *IL-32 Drives the Differentiation of Cardiotropic CD4+ T-Cells Carrying HIV DNA in People Living with HIV.* J Infect Dis, 2023.

69. Rothan, C., et al., *Antiretroviral therapy-treated HIV-infected adults with coronary artery disease are characterized by a distinctive regulatory T-cell signature.* AIDS, 2021. **35**(7): p. 1003-1014.

70. Gui, Y., et al., *Development and function of natural TCR(+) CD8alphaalpha(+) intraepithelial lymphocytes.* Front Immunol, 2022. **13**: p. 1059042.

71. Hu, M.D., L. Jia, and K.L. Edelblum, *Policing the intestinal epithelial barrier: Innate immune functions of intraepithelial lymphocytes.* Curr Pathobiol Rep, 2018. **6**(1): p. 35-46.

72. Nielsen, M.M., D.A. Witherden, and W.L. Havran, *gammadelta T cells in homeostasis and host defence of epithelial barrier tissues.* Nat Rev Immunol, 2017. **17**(12): p. 733-745.

73. Turcotte, I., et al., *Association Between the Development of Subclinical Cardiovascular Disease and Human Immunodeficiency Virus (HIV) Reservoir Markers in People With HIV on Suppressive Antiretroviral Therapy.* Clin Infect Dis, 2023. **76**(7): p. 1318-1321.

74. Folsom, A.R., et al., *Plasma d-Dimer and Incident Ischemic Stroke and Coronary Heart Disease: The Atherosclerosis Risk in Communities Study.* Stroke, 2016. **47**(1): p. 18-23.

75. Tibaut, M., et al., *Markers of Atherosclerosis: Part 1 - Serological Markers.* Heart Lung Circ, 2019. **28**(5): p. 667-677.

76. Planas, D., et al., *LILAC pilot study: Effects of metformin on mTOR activation and HIV reservoir persistence during antiretroviral therapy.* EBioMedicine, 2021. **65**: p. 103270.

77. Zaunders, J., et al., *CD4(+) T Follicular Helper and IgA(+) B Cell Numbers in Gut Biopsies from HIV-Infected Subjects on Antiretroviral Therapy Are Similar to HIV-Uninfected Individuals.* Front Immunol, 2016. **7**: p. 438.

78. Mayassi, T., et al., *A multilayered immune system through the lens of unconventional T cells.* Nature, 2021. **595**(7868): p. 501-510.

79. Ziegler, H., et al., *Human Peripheral CD4(+) Vdelta1(+) gammadeltaT Cells Can Develop into alphabetaT Cells.* Front Immunol, 2014. **5**: p. 645.

80. Li, H. and C.D. Pauza, *HIV envelope-mediated, CCR5/alpha4beta7-dependent killing of CD4-negative gammadelta T cells which are lost during progression to AIDS.* Blood, 2011. **118**(22): p. 5824-31.

81. Pauza, C.D., et al., *gammadelta T Cells in HIV Disease: Past, Present, and Future.* Front Immunol, 2014. **5**: p. 687.

82. Walker, E.M., et al., *Dysregulation of IL-17/IL-22 Effector Functions in Blood and Gut Mucosal Gamma Delta T Cells Correlates With Increase in Circulating Leaky Gut and Inflammatory Markers During cART-Treated Chronic SIV Infection in Macaques.* Front Immunol, 2021. **12**: p. 647398.

83. Cibrian, D. and F. Sanchez-Madrid, *CD69: from activation marker to metabolic gatekeeper.* Eur J Immunol, 2017. **47**(6): p. 946-953.

84. Radulovic, K. and J.H. Niess, *CD69 is the crucial regulator of intestinal inflammation: a new target molecule for IBD treatment?* J Immunol Res, 2015. **2015**: p. 497056.

85. Thome, J.J. and D.L. Farber, *Emerging concepts in tissue-resident T cells: lessons from humans.* Trends Immunol, 2015. **36**(7): p. 428-35.

86. Couturier, J., et al., *Human adipose tissue as a reservoir for memory CD4+ T cells and HIV.* AIDS, 2015. **29**(6): p. 667-74.

87. Wanjalla, C.N., et al., *Adipose Tissue in Persons With HIV Is Enriched for CD4(+) T Effector Memory and T Effector Memory RA(+) Cells, Which Show Higher CD69 Expression and CD57, CX3CR1, GPR56 Co-expression With Increasing Glucose Intolerance.* Front Immunol, 2019. **10**: p. 408.

88. Wang, X., et al., *Distinct expression patterns of CD69 in mucosal and systemic lymphoid tissues in primary SIV infection of rhesus macaques.* PLoS One, 2011. **6**(11): p. e27207.

89. Alvarez, Y., et al., *Preferential HIV infection of CCR6+ Th17 cells is associated with higher levels of virus receptor expression and lack of CCR5 ligands.* J Virol, 2013. **87**(19): p. 10843-54.

90. Lee, A.Y.S. and H. Korner, *CCR6/CCL20 chemokine axis in human immunodeficiency virus immunity and pathogenesis.* J Gen Virol, 2017. **98**(3): p. 338-344.

91. Khoury, G., et al., *Persistence of integrated HIV DNA in CXCR3 + CCR6 + memory CD4+ T cells in HIV-infected individuals on antiretroviral therapy.* AIDS, 2016. **30**(10): p. 1511-20.

92. Gosselin, A., et al., *HIV persists in CCR6+CD4+ T cells from colon and blood during antiretroviral therapy.* AIDS, 2017. **31**(1): p. 35-48.

93. Anderson, J.L., et al., *Human Immunodeficiency Virus (HIV)-Infected CCR6+ Rectal CD4+ T Cells and HIV Persistence On Antiretroviral Therapy.* J Infect Dis, 2020. **221**(5): p. 744-755.

94. Xu, W., T. Bergsbaken, and K.L. Edelblum, *The multifunctional nature of CD103 (alphaEbeta7 integrin) signaling in tissue-resident lymphocytes.* Am J Physiol Cell Physiol, 2022. **323**(4): p. C1161-C1167.

95. Vimonpatranon, S., et al., *MAdCAM-1 costimulation in the presence of retinoic acid and TGF-beta promotes HIV infection and differentiation of CD4+ T cells into CCR5+ TRM-like cells.* PLoS Pathog, 2023. **19**(3): p. e1011209.

96. Wu, X., et al., *The Roles of CCR9/CCL25 in Inflammation and Inflammation-Associated Diseases.* Front Cell Dev Biol, 2021. **9**: p. 686548.

97. Nakayama, M., et al., *Shaping of T Cell Functions by Trogocytosis.* Cells, 2021. **10**(5).

98. Schriek, P. and J.A. Villadangos, *Trogocytosis and cross-dressing in antigen presentation.* Curr Opin Immunol, 2023. **83**: p. 102331.

99. Kant, S., et al., *Polyfunctional Fc Dependent Activity of Antibodies to Native Trimeric Envelope in HIV Elite Controllers.* Front Immunol, 2020. **11**: p. 583820.

100. Vo, D.N., et al., *NK Cells Acquire CCR5 and CXCR4 by Trogocytosis in People Living with HIV-1.* Vaccines (Basel), 2022. **10**(5).

101. Mattapallil, J.J., E. Reay, and S. Dandekar, *An early expansion of CD8alphabeta T cells, but depletion of resident CD8alphaalpha T cells, occurs in the intestinal epithelium during primary simian immunodeficiency virus infection.* AIDS, 2000. **14**(6): p. 637-46.

102. Sun, Z., et al., *Intrarectal transmission, systemic infection, and CD4+ T cell depletion in humanized mice infected with HIV-1.* J Exp Med, 2007. **204**(4): p. 705-14.

103. Konno, A., et al., *CD8alpha alpha memory effector T cells descend directly from clonally expanded CD8alpha +beta high TCRalpha beta T cells in vivo.* Blood, 2002. **100**(12): p. 4090-7.

104. Ma, H., Y. Qiu, and H. Yang, *Intestinal intraepithelial lymphocytes: Maintainers of intestinal immune tolerance and regulators of intestinal immunity.* J Leukoc Biol, 2021. **109**(2): p. 339-347.

105. Knezovic, A., et al., *Role of Oxidative Stress in Vascular Low-Grade Inflammation Initiation Due to Acute Salt Loading in Young Healthy Individuals.* Antioxidants (Basel), 2022. **11**(3).

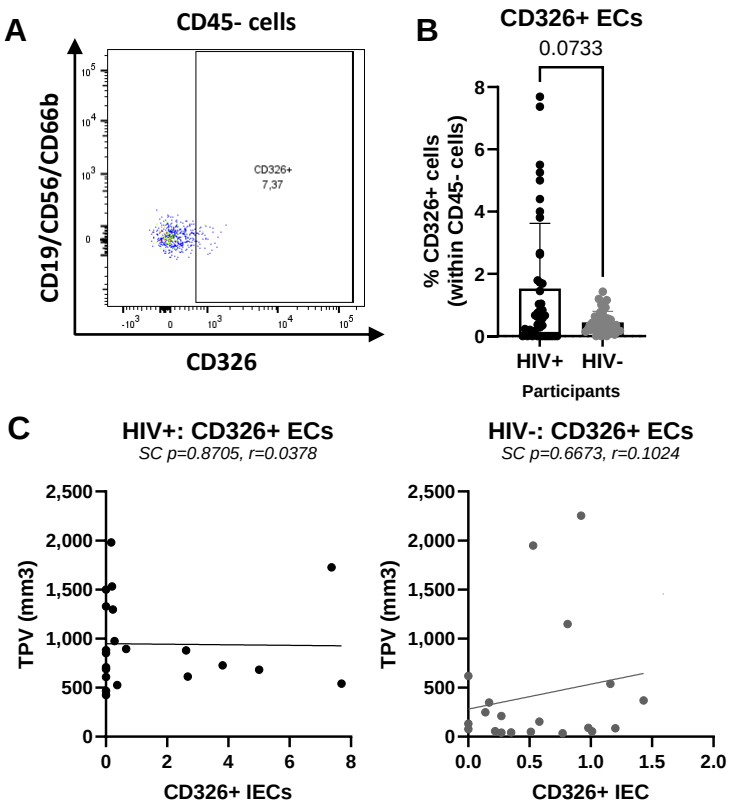

Moreira Gabriel et al., Figure 1

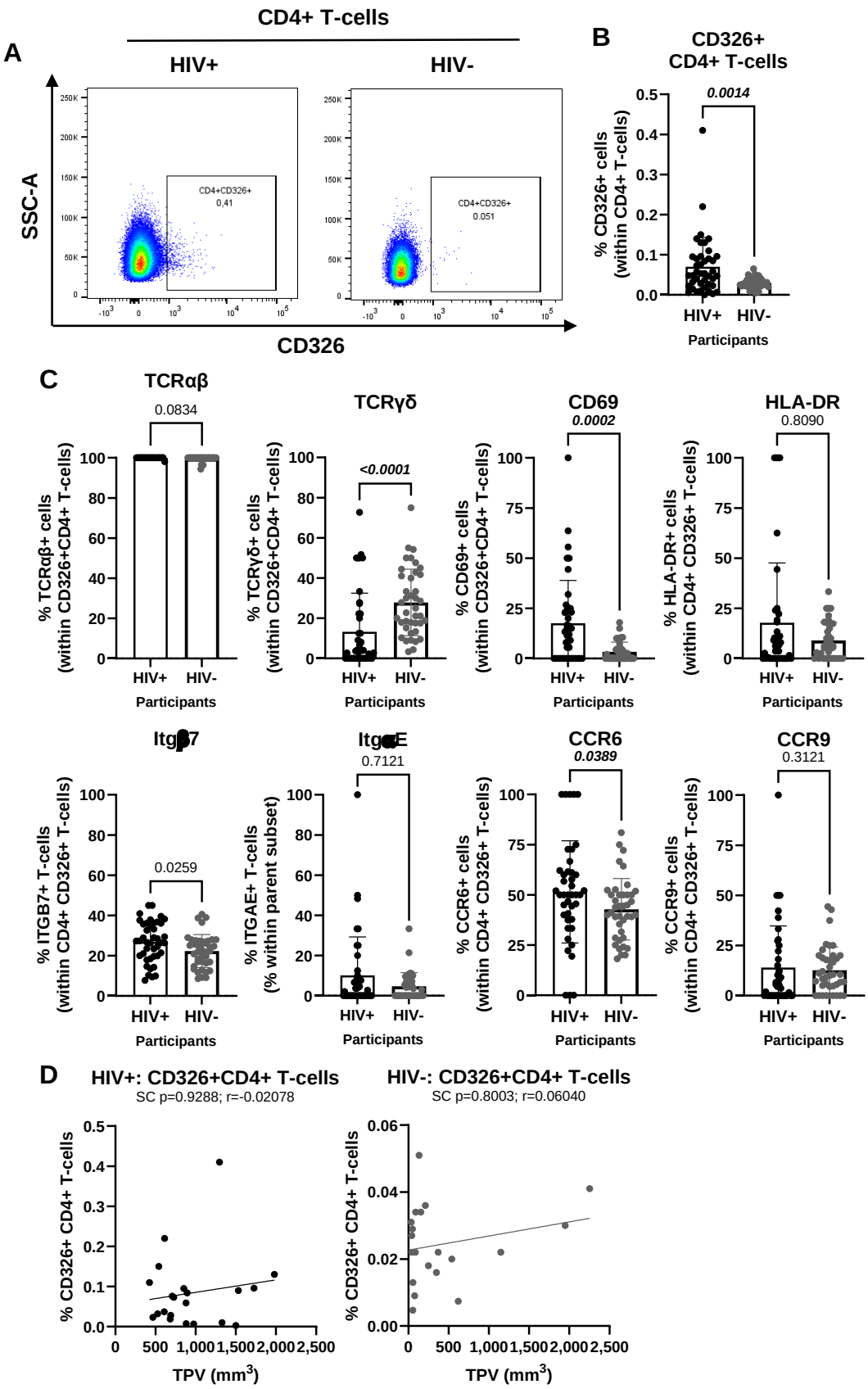

Moreira Gabriel et al., Figure 2

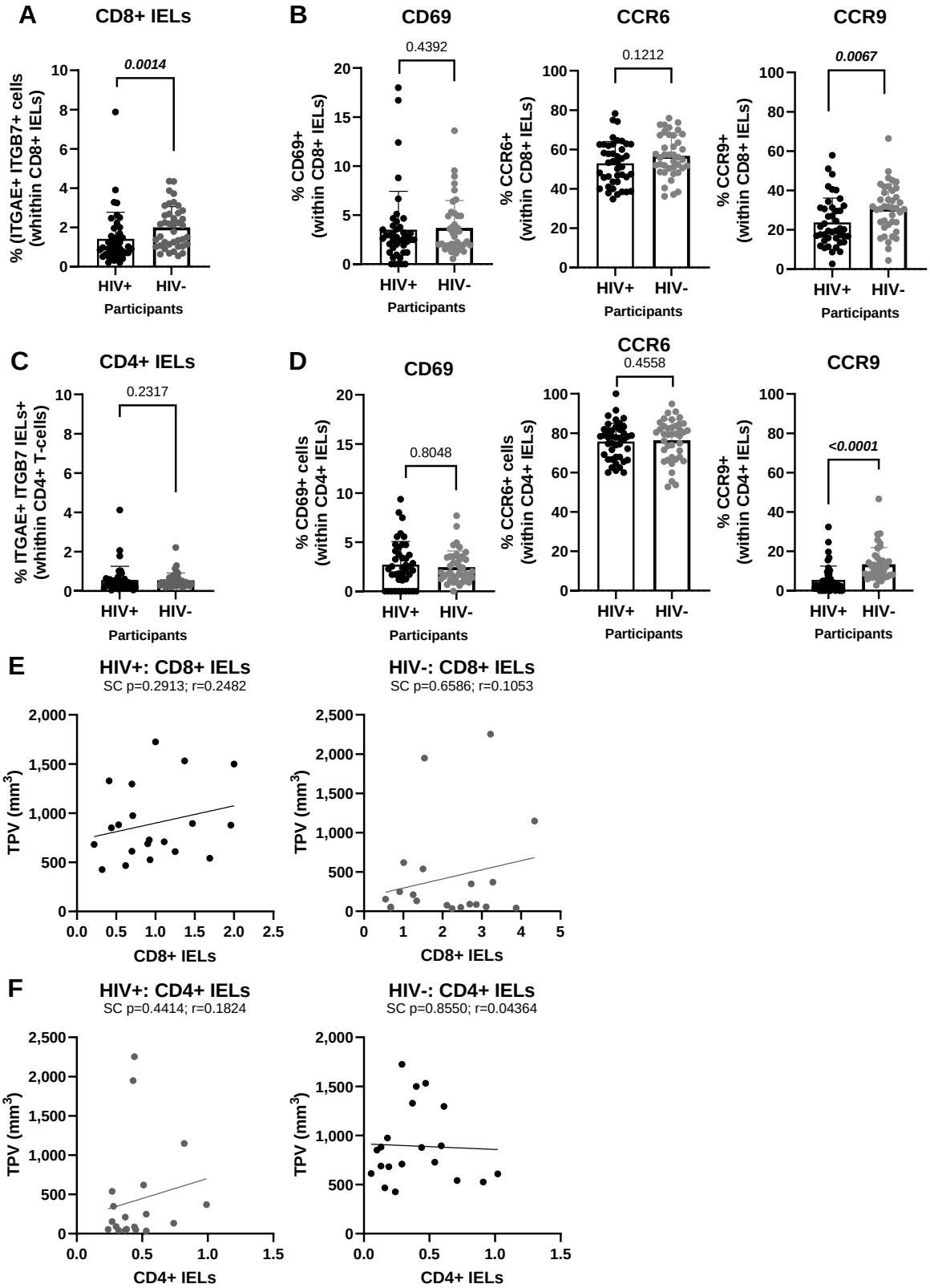

Moreira Gabriel et al., Figure 3

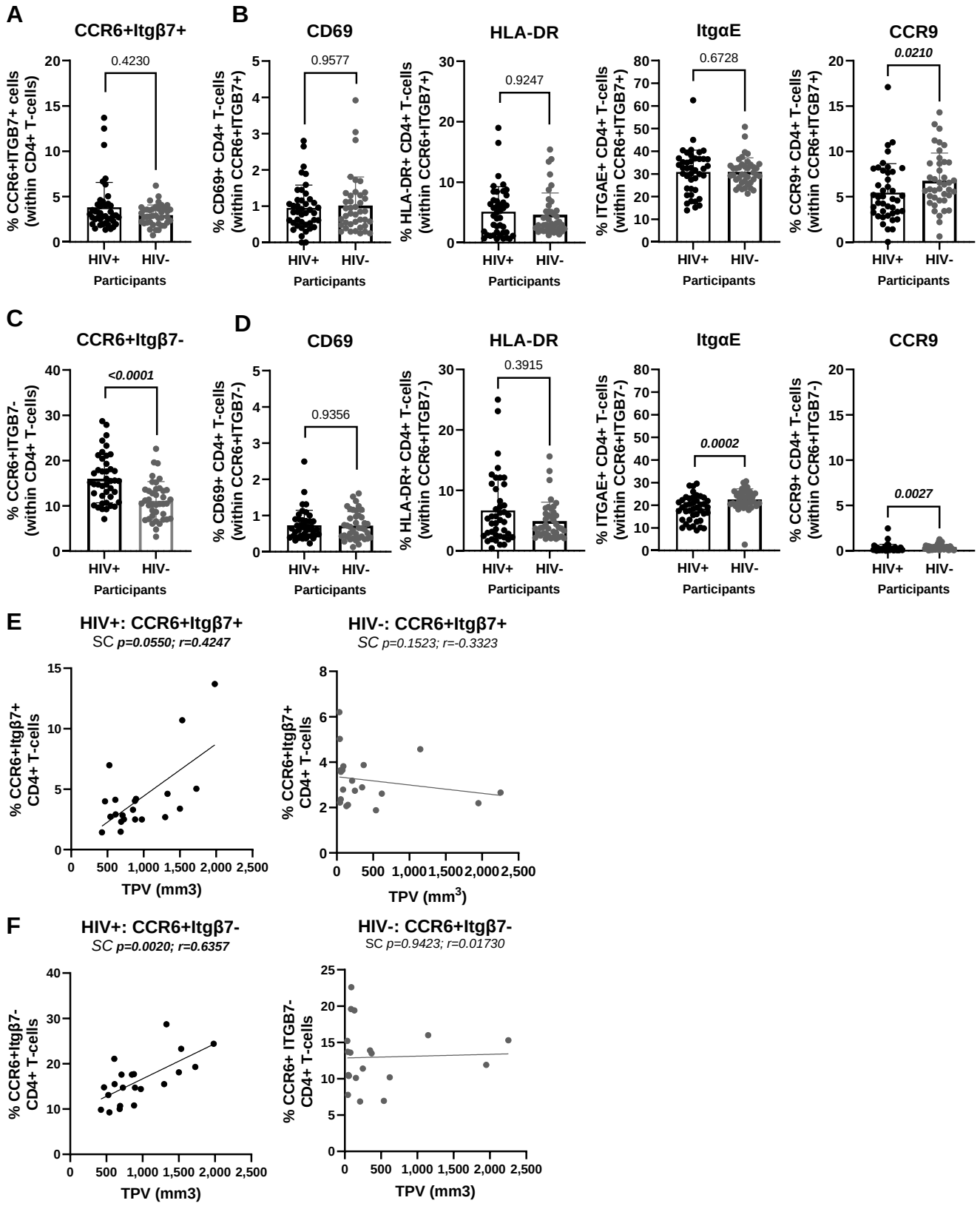

Moreira Gabriel et al., Figure 4